

High-Mobility n-Type Conjugated Polymers Based on Electron-Deficient Tetraazabenzodifluoranthene Diimide for Organic Electronics

Haiyan Li, Felix Sunjoo Kim,[†] Guoqiang Ren, and Samson A. Jenekhe*

Department of Chemical Engineering and Department of Chemistry, University of Washington, Seattle, Washington 98195-1750, United States

S Supporting Information

ABSTRACT: High-mobility p-type and ambipolar conjugated polymers have been widely reported. However, high-mobility n-type conjugated polymers are still rare. Herein we present poly(tetraazabenzodifluoranthene diimide)s, PBFI-T and PBFI-BT, which exhibit a novel two-dimensional (2D) π -conjugation along the main chain and in the lateral direction, leading to high-mobility unipolar n-channel transport in field-effect transistors. The n-type polymers exhibit electron mobilities of up to 0.30 cm²/(V s), which is among the highest values for unipolar n-type conjugated polymers. Complementary inverters incorporating n-channel PBFI-T transistors produced nearly perfect switching characteristics with a high gain of 107.

Conjugated polymers are ideal semiconductors for next generation low-cost electronics in part because they combine interesting tunable electronic and optical properties with excellent solution processing and mechanical flexibility.¹ Facile injection and transport of charge carriers, both electrons and holes, in semiconducting polymers are critical factors that determine the achievable performance of organic electronics.¹ Envisioned low power complementary circuits composed of n-channel organic field-effect transistors (OFETs) and p-channel OFETs are necessarily made from two different types of semiconducting polymers, electron-transport (n-type) and hole-transport (p-type) materials.^{1,2} Compared to the plethora of solution processable p-type conjugated polymers now available with high hole mobility,^{2a,3} very few high-mobility n-type polymer semiconductors have been reported.⁴ The development of solution processable high-mobility n-type semiconducting polymers remains a major obstacle to further advances in organic electronics.^{1,2b,e,g}

High-mobility n-type semiconducting polymers are scarce because of several scientific challenges. Suitable electron-deficient building blocks or monomers, which can yield polymers with high electron affinity or a low-lying lowest unoccupied molecular orbital (LUMO) energy level essential to facile injection of electrons, are few.^{1b,c,2d,e,g} Such n-type conjugated polymers also require high ionization energy or a low-lying highest occupied molecular orbital (HOMO) energy level to suppress facile injection of holes and thus ambipolar charge transport.^{1a,2a,5} Electron-deficient monomers are more difficult to controllably polymerize to high molecular weights

than well-studied electron-rich monomers used for p-type polymers.^{4e,f} Copolymerization of electron-deficient monomers with an electron-rich one frequently results in p-type or ambipolar polymers.⁵ Highly planar chain segments, strong intermolecular interactions, and ordered molecular packing necessary for efficient charge transport are often incompatible with requirements for solubility and solution processability.^{4a}

In this paper, we report a novel π -conjugated macromolecular architecture composed of an 11-ring polycyclic chromophore, *N,N'*-bis(2-decyltetradecyl)-tetraazabenzodifluoranthene diimide (BFI),⁶ as the key building block. Our recent study of the monomeric BFI system showed that it was planar, had a 2.0 nm long π -conjugated framework, had a high electron affinity, and exhibited strong intermolecular interactions.⁶ We herein demonstrate that embedding of the rigid BFI building block into a polymer main chain creates a well-defined lateral extension of π -electron delocalization in addition to the π -conjugated main-chain spine. The resulting poly(tetraazabenzodifluoranthene diimide)s (PBFI)s are found to exhibit high-mobility electron transport in n-channel transistors and to facilitate the creation of complementary electronic circuits with nearly ideal switching characteristics.

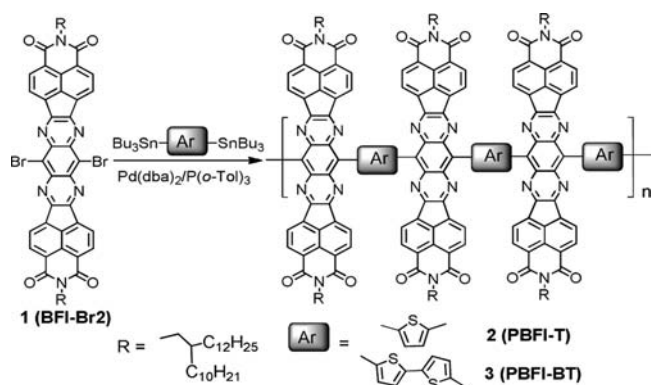
The new n-type conjugated polymers, including the thiophene-linked (PBFI-T) and the bithiophene-linked (PBFI-BT) derivatives, were synthesized by Stille cross-coupling polymerization (Scheme 1).⁷ PBFI-T had excellent solubility in organic solvents (e.g., chloroform, toluene, and chlorobenzene) whereas PBFI-BT was not very soluble in these solvents. The number- and weight-average molecular weights (M_n , M_w) of PBFI-T, determined by gel chromatography against polystyrene standards, were 48 and 175 kDa with a polydispersity index (M_w/M_n) of 3.68. Both polymers had excellent thermal stability with an onset thermal decomposition temperature of 450 °C and 43–48% weight remaining at 800 °C in nitrogen under thermogravimetric analysis (Figure S1). Melting or glass transition was not observed in the 20–400 °C range of differential scanning calorimetry scans. These rugged thermal stability characteristics of the PBFI)s are reminiscent of those of ladder polymers.^{4a}

Optical absorption spectroscopy provides insight into the electronic structure of the new conjugated polymers. The monomeric chromophore BFI thin film has a main absorption

Received: July 21, 2013

Published: September 25, 2013

Scheme 1. Synthesis of PBFI s including PBFI-T and PBFI-BT



band centered at 360 nm due to the π - π^* transition.⁶ In contrast, both polymers retain this high energy band with a peak at \sim 380 nm while exhibiting a new, broad, lower energy band at 500–950 nm for PBFI-T and 600–1300 nm for PBFI-BT, respectively (Figure 1). Emergence of the new lower

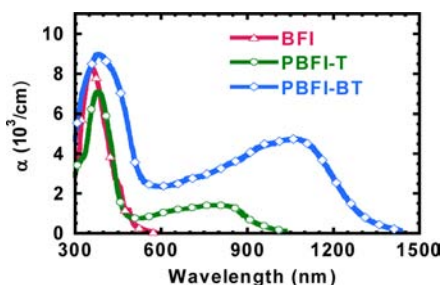


Figure 1. Optical absorption spectra of BFI, PBFI-T, and PBFI-BT thin films on glass substrates.

energy absorption band in PBFI-T and PBFI-BT confirms electronic delocalization along the chain axis, which is enhanced by intramolecular charge transfer (ICT) between the electron-deficient BFI unit and the electron-donating thiophene or bithiophene ring.^{7,8} The ICT character of this absorption band also explains why it is red-shifted and its oscillator strength is larger in PBFI-BT compared to PBFI-T since bithiophene is a stronger electron-donating unit than thiophene. Optical absorption edge band gaps of 1.29 and 0.94 eV were obtained for PBFI-T and PBFI-BT, respectively, from the thin film absorption spectra (Figure 1). Reduction and oxidation cyclic voltammetry of the polymer thin films provided additional characterization of the electronic structure (Figure S3), yielding LUMO/HOMO energy levels of $-3.80/-5.45$ eV and $-3.74/-5.14$ eV for PBFI-T and PBFI-BT, respectively (Table S1).

X-ray diffraction (XRD) analysis of drop cast PBFI-T and PBFI-BT films on glass substrates provided ordering and molecular packing information on the polymers in the solid state. The reflections of PBFI-T at 3.3° and 6.5° indexed as the (100) plane and its weak second order (200) reflection, respectively, suggested a lamellar crystalline ordering with a d -spacing of 2.6 nm (Figure 2a). A weak reflection at 11.3° , which intensified by tilting the substrate from 90° to 54.5° (Figure S4) corresponds to a d -spacing of \sim 0.8 nm due to the diffraction of the repeating unit along the polymer chain. A broad weak peak at 20.9° with a d -spacing of 0.4 nm arises from weak π - π stacking of the polymer. The (100) and

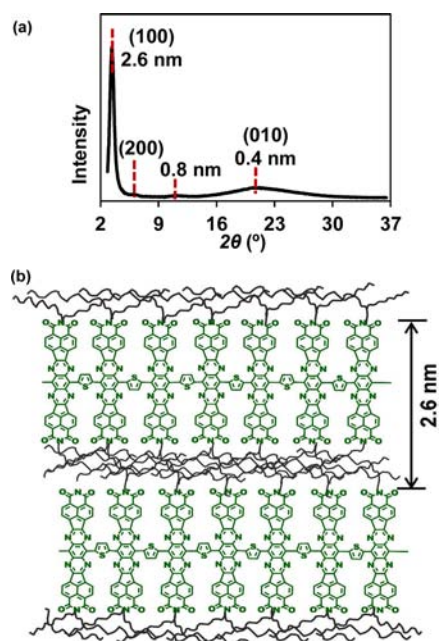


Figure 2. (a) XRD patterns of drop-cast PBFI-T film on a glass substrate after annealing at 250°C . (b) Schematic illustration of the lamellar ordered structure of PBFI-T deduced from the XRD patterns.

corresponding (200) reflections of PBFI-BT were found at 2.88° and 5.62° , respectively, corresponding to a larger lamellar d -spacing of 3.1 nm than that of PBFI-T (Figure S5). Weak broad diffraction at 26.1° due to π - π stacking corresponds to a distance of 0.35 nm, which is significantly shorter than that of PBFI-T as a result of better coplanarity of PBFI-BT. An unusual feature of the observed lamellar crystalline structure is the very small space occupied by the insulating and solubilizing alkyl side chains between the rigid π -conjugated framework (Figure 2b),⁹ an important consequence of the large lateral π -conjugation length (\sim 2.0 nm)⁶ of this class of conjugated polymers.

The unusual lamellar structure of PBFI-T and PBFI-BT chains was further investigated by high resolution transmission electron microscopy (HRTEM). One- and few-monolayer thin film samples of PBFI-T and PBFI-BT on 300 mesh lacey-carbon-coated copper grids were imaged at 200 kV (Figures S6 and S7). HRTEM images revealed widths of 1.5–2.0 nm, which corresponds to the conjugated width of the nanoribbon-like polymer chains (Figures S6b, 6c and S7b); longer polymer chains could not be observed likely because of overlapping chains, molecular mobility, and resolution limitations of the instrument. Selected area electron diffraction (SAED) revealed a lamellar crystalline ordering of the few-monolayer PBFI-T films (Figure S6 inset), from which the (200) and (010) electron diffractions corresponding to d -spacings of 2.4 and 0.87 nm were observed in close agreement with the above X-ray diffraction results (Figure S9).

We fabricated and evaluated thin film OFETs in nitrogen to study the charge transport properties of PBFI-T and PBFI-BT. The bottom-gate and top-contact transistors were fabricated on silicon/silicon dioxide substrates, and the surface of the SiO₂ gate dielectric was hydrophobically modified by either a monolayer of octyltrichlorosilane (OTS8) or a polymer dielectric thin film such as the fluoropolymer CYTOP or cross-linked benzocyclobutene (BCB). Figure 3a and 3b show

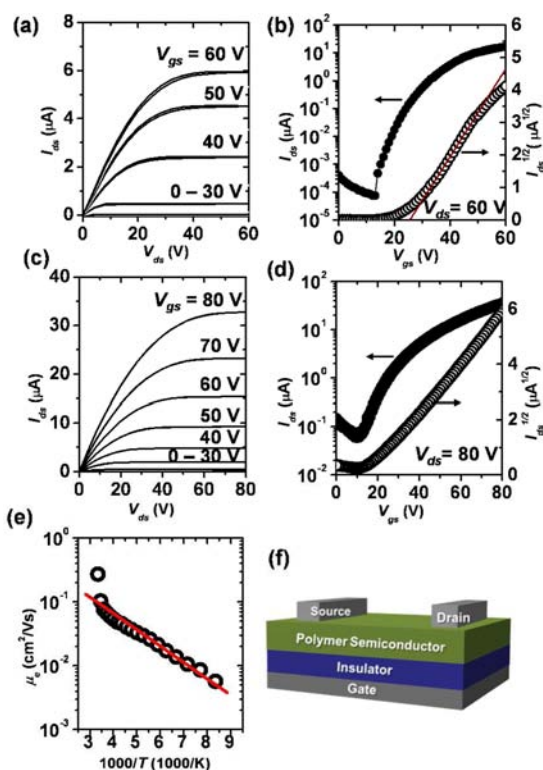


Figure 3. Current–voltage output and transfer curves of (a and b) PBFI-T transistors with Ag source–drain electrodes on an OTS8-treated substrate; (c and d) PBFI-T transistors with Ag source–drain electrodes on a CYTOP-coated substrate; (e) electron mobility versus inverse temperature with least-squares fitting of the data to the Arrhenius equation ($\mu = \mu_0 \exp(-E_A/k_B T)$); (f) Schematic of bottom-gate/top-contact transistors.

the output curves and transfer characteristics, respectively, of n-channel OFETs consisting of PBFI-T thin films on OTS8 and silver (Ag) source–drain electrodes. PBFI-T devices annealed at 200 °C had a high saturation region electron mobility of 0.30 $\text{cm}^2/(\text{V s})$ (0.18 $\text{cm}^2/(\text{V s})$ average of 16 devices fabricated in 4 batches) with excellent current modulation (10^5 – 10^6), which is among the highest mobilities for n-type conjugated polymers.^{4a–c,f} PBFI-T OFETs with a CYTOP buffer layer (Figure 3c and 3d) also showed ideal linear and saturation characteristics but had a lower electron mobility of 0.11–0.13 $\text{cm}^2/(\text{V s})$. In contrast to the PBFI-T OFETs, the best PBFI-BT transistors were on the BCB-modified dielectric (Figure S10) and they gave a saturation electron mobility of 0.09 $\text{cm}^2/(\text{V s})$ with moderate on/off current ratios (10^3 – 10^4). The significantly lower performance of PBFI-BT n-channel OFETs compared to those of PBFI-T is due largely to the poor solubility and poor quality of its spin-coated thin films.

Temperature-dependent charge transport measurements on PBFI-T transistors provided insight into the high electron mobility. The thermally activated nature of electron transport in PBFI-T is confirmed by the temperature dependent I – V curves of the PBFI-T transistor (Figure S11a). A plot of electron mobility as a function of inverse temperature is overlaid with Arrhenius-type fitting to the equation $\mu = \mu_0 \exp(-E_A/k_B T)$ (Figure 3e). The observed Arrhenius-type dependence originates from trapping events of charge carriers in localized states, which are present at the interfacial imperfections and/or at the boundaries of high-mobility domains, in thin films of organic semiconductors.¹⁰ The

observed pre-exponential constant μ_0 of 0.7 $\text{cm}^2/(\text{V s})$ and low activation energy E_A of 50.9 meV obtained from the fitting imply that the intrinsic electron mobility of PBFI-T is much higher than we obtained from the device. Switching from the OTS8- to CYTOP-modified gate dielectric slightly reduced the parameters to $\mu_0 = 0.4 \text{ cm}^2/(\text{V s})$ and $E_A = 43.8 \text{ meV}$ (Figure S11b and S11c). The observed activation energy of 44–51 meV is similar to or lower than the 44–85 meV seen in other high-mobility n-type polymer semiconductors, suggesting that the electronic energy levels for charge transport are close to the Fermi level under on-state conditions of the OFETs and that there is a rather low density of deep trapping sites in PBFI-T thin films.¹⁰

Complementary inverters based on n-channel PBFI-T OFETs were fabricated and evaluated to explore their potential for developing complementary polymer electronic circuits (Figure 4a).^{2c} The needed p-channel OFETs were fabricated

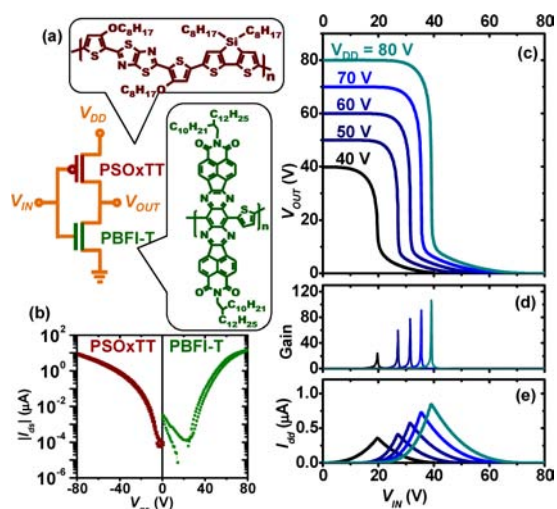


Figure 4. (a) Schematic of a complementary p/n polymer inverter and molecular structures of p-channel polymer PSOxTT and n-channel polymer PBFI-T. (b) Transfer curves of the p-channel and n-channel polymer transistors. Static switching characteristics of the inverter: (c) output voltage, (d) gain, and (e) current as a function of input voltage (V_{IN}) with various power supply voltages (V_{DD}).

from the semiconducting polymer poly[(4,4'-bis(2-octyl)-dithieno[3,2-*b*:2',3'-*d*]silole)-2,6-diyl-alt-(2,5-bis(3-octyloxythiophen-2yl)thiazolo[5,4-*d*]thiazole) (PSOxTT), which has a reported hole mobility of 0.1 $\text{cm}^2/(\text{V s})$.¹¹ The I – V curves of the constituent PBFI-T and PSOxTT OFETs show comparable on-current and off-current (Figure 4b). Inverters fabricated with the same device architecture (i.e., OTS8-treated 200-nm-thick SiO_2 and gold electrodes with channel width/length = 10) for both OFETs have an ideal switching behavior (Figure 4c, 4d, and 4e). The switching voltage was nearly at half of the supply voltage ($V_{IN} - V_{DD}/2$). The transition of the complementary inverter was also very sharp with the voltage gain ($-dV_{OUT}/dV_{IN}$) as high as 107, resulting in the large noise tolerance of the circuits. The amount of current (I_{DD}) flowing through the complementary inverter, and thus its power consumption, is only high (0.84 μA , or 67 μW , at $V_{DD} = 80 \text{ V}$) when the circuit is under active switching. In the static state, I_{DD} was less than 19 nA (i.e., power less than 1.5 μW) when $V_{DD} = 80 \text{ V}$. The power consumption could be further significantly

reduced compared to this value by the use of recently developed low-voltage OFET methodology.¹²

In summary, new n-type π -conjugated polymers with a large lateral extension (2.0 nm) of π -conjugation were realized by embedding a tetraazabenzodifluoranthene diimide building block into a polymer chain and the unusual lamellar ordering was confirmed by XRD. The novel class of π -conjugated polymers provides a new approach to high-mobility electron transport in polymer semiconductors. The observed electron mobilities of up to 0.30 cm²/(V s) for PBFI-T are among the highest to date for n-channel polymer transistors. The temperature-dependent charge transport measurements indicated a low density of deep trapping sites. n-Channel transistors based on PBFI-T enabled the fabrication of high-gain complementary inverters with nearly ideal switching characteristics.

■ ASSOCIATED CONTENT

📄 Supporting Information

Experimental details and characterization data. This material is available free of charge via the Internet at <http://pubs.acs.org>.

■ AUTHOR INFORMATION

Corresponding Author

jenekhe@u.washington.edu

Present Address

[†]Department of Chemical Engineering and Materials Science, Chung-Ang University, Seoul, Korea.

Notes

The authors declare no competing financial interest.

■ ACKNOWLEDGMENTS

The design and synthesis of n-type conjugated polymers were supported by the NSF (DMR-1035196), Office of Naval Research (ONR) (N00014-11-1-0317), and Solvay S. A. Studies of charge transport were supported by the Boeing-Martin Professorship.

■ REFERENCES

- (1) (a) Zaumseil, J.; Sirringhaus, H. *Chem. Rev.* **2007**, *107*, 1296. (b) Facchetti, A. *Chem. Mater.* **2011**, *23*, 733. (c) Newman, C. R.; Frisbie, C. D.; da Silva Filho, D. A.; Brédas, J.-L.; Ewbank, P. C.; Mann, K. R. *Chem. Mater.* **2004**, *16*, 4436.
- (2) (a) Wang, C.; Dong, H.; Hu, W.; Liu, Y.; Zhu, D. *Chem. Rev.* **2012**, *112*, 2208. (b) Usta, H.; Facchetti, A.; Marks, T. J. *Acc. Chem. Res.* **2011**, *44*, 501. (c) Klauk, H.; Zschieschang, U.; Pflaum, J.; Halik, M. *Nature* **2007**, *445*, 745. (d) Crone, B.; Dodabalapur, A.; Lin, Y. Y.; Filas, R. W.; Bao, Z.; LaDuca, A.; Sarpeshkar, R.; Katz, H. E.; Li, W. *Nature* **2000**, *403*, 521. (e) Anthony, J. E.; Facchetti, A.; Heeney, M.; Marder, S. R.; Zhan, X. *Adv. Mater.* **2010**, *22*, 3876. (f) Briseno, A. L.; Kim, F. S.; Babel, A.; Xia, Y.; Jenekhe, S. A. *J. Mater. Chem.* **2011**, *21*, 16461. (g) Zhao, X.; Zhan, X. *Chem. Soc. Rev.* **2011**, *40*, 3728.
- (3) (a) Li, J.; Zhao, Y.; Tan, H. S.; Guo, Y.; Di, C.-A.; Yu, G.; Liu, Y.; Lin, M.; Lim, S. H.; Zhou, Y.; Su, H.; Ong, B. S. *Sci. Rep.* **2012**, *2*. (b) Tsao, H. N.; Cho, D. M.; Park, I.; Hansen, M. R.; Mavrinskiy, A.; Yoon, D. Y.; Graf, R.; Pisula, W.; Spiess, H. W.; Müllen, K. *J. Am. Chem. Soc.* **2011**, *133*, 2605. (c) Chen, H.; Guo, Y.; Yu, G.; Zhao, Y.; Zhang, J.; Gao, D.; Liu, H.; Liu, Y. *Adv. Mater.* **2012**, *24*, 4589.
- (4) (a) Babel, A.; Jenekhe, S. A. *J. Am. Chem. Soc.* **2003**, *125*, 13656. (b) Yan, H.; Chen, Z.; Zheng, Y.; Newman, C.; Quinn, J. R.; Dötz, F.; Kastler, M.; Facchetti, A. *Nature* **2009**, *457*, 679. (c) Guo, X.; Ortiz, R. P.; Zheng, Y.; Hu, Y.; Noh, Y.-Y.; Baeg, K.-J.; Facchetti, A.; Marks, T. J. *J. Am. Chem. Soc.* **2011**, *133*, 1405. (d) Takeda, Y.; Andrew, T. L.; Lobez, J. M.; Mork, A. J.; Swager, T. M. *Angew. Chem., Int. Ed.* **2012**,

51, 9042. (e) Lee, J.-K.; Gwinner, M. C.; Berger, R.; Newby, C.; Zentel, R.; Friend, R. H.; Sirringhaus, H.; Ober, C. K. *J. Am. Chem. Soc.* **2011**, *133*, 9949. (f) Lei, T.; Dou, J.-H.; Cao, X.-Y.; Wang, J.-Y.; Pei, J. *J. Am. Chem. Soc.* **2013**, *135*, 12168.

(5) (a) Kim, F. S.; Guo, X.; Watson, M. D.; Jenekhe, S. A. *Adv. Mater.* **2010**, *22*, 478. (b) Guo, X.; Kim, F. S.; Seger, M. J.; Jenekhe, S. A.; Watson, M. D. *Chem. Mater.* **2012**, *24*, 1434. (c) Usta, H.; Facchetti, A.; Marks, T. J. *J. Am. Chem. Soc.* **2008**, *130*, 8580.

(6) Li, H.; Kim, F. S.; Ren, G.; Hollenbeck, E. C.; Subramanian, S.; Jenekhe, S. A. *Angew. Chem., Int. Ed.* **2013**, *52*, 5513.

(7) Zhu, Y.; Champion, R. D.; Jenekhe, S. A. *Macromolecules* **2006**, *39*, 8712.

(8) Jenekhe, S. A.; Lu, L.; Alam, M. M. *Macromolecules* **2001**, *34*, 7315.

(9) Mei, J.; Kim, D. H.; Ayzner, A. L.; Toney, M. F.; Bao, Z. *J. Am. Chem. Soc.* **2011**, *133*, 20130.

(10) (a) Caironi, M.; Bird, M.; Fazzi, D.; Chen, Z.; Di Pietro, R.; Newman, C.; Facchetti, A.; Sirringhaus, H. *Adv. Funct. Mater.* **2011**, *21*, 3371. (b) Meijer, E. J.; Matters, M.; Herwig, P. T.; de Leeuw, D. M.; Klapwijk, T. M. *Appl. Phys. Lett.* **2000**, *76*, 3433. (c) Sirringhaus, H.; Brown, P. J.; Friend, R. H.; Nielsen, M. M.; Bechgaard, K.; Langeveld-Voss, B. M. W.; Spiering, A. J. H.; Janssen, R. A. J.; Meijer, E. W.; Herwig, P.; de Leeuw, D. M. *Nature* **1999**, *401*, 685.

(11) Subramanian, S.; Xin, H.; Kim, F. S.; Shoaee, S.; Durrant, J. R.; Jenekhe, S. A. *Adv. Energy Mater.* **2011**, *1*, 854.

(12) Cho, J. H.; Lee, J.; Xia, Y.; Kim, B.; He, Y.; Renn, M. J.; Lodge, T. P.; Frisbie, C. D. *Nat. Mater.* **2008**, *7*, 900.